# Modelling of tritium retention and target lifetime of the ITER divertor using the ERO code

A. Kirschner [a,*], D. Borodin [a], S. Droste [a], V. Philipps [a], U. Samm [a],
G. Federici [b], A. Kukushkin [b], A. Loarte [c]

[a] *Institut für Plasmaphysik, Forschungszentrum Jülich, Association EURATOM-FZJ, Trilateral Euregio Cluster, Germany*
[b] *ITER JWS Garching Co Center, Boltzmannstrasse 2, D-85748 Garching, Germany*
[c] *European Fusion Development Agreement, Close Support Unit, D-85748 Garching, Germany*

## Abstract

Material erosion, transport and deposition in the divertor of ITER are modelled with the Monte-Carlo impurity transport code ERO taking into account chemical erosion, physical sputtering, enhanced chemical erosion of redeposited carbon and a beryllium influx from main chamber erosion. The continuous deposition of beryllium leads to reduced carbon erosion along the divertor plates with increasing exposure time. With 1% beryllium in the edge plasma an upper value of the long-term tritium retention rate can be estimated to about 15.9 mg T/s. For 0.1% beryllium this number decreases to about 6.4 mg T/s. These numbers do not change significantly with the sticking assumption for hydrocarbons. The erosion of the divertor plates is less critical. Maximal erosion rates of 0.4 nm/s with 1% beryllium and 1.8 nm/s with 0.1% beryllium occur at the outer target. Erosion due to transient heat loads is not yet included in the modelling.

## 1. Introduction

In the design of ITER [1], carbon fibre composites (CFC) are foreseen for the divertor target plates where the highest heat loads are expected. The advantage of non-melting of graphite materials opposes their strong erosion due to chemical formation of hydrocarbon molecules even at low plasma temperatures. Extrapolations from current experiments to ITER indicate a critical amount of tritium retention due to co-deposition. However, experimental data are based on full-carbon-clad devices, whereas in ITER beryllium is foreseen for the main wall and tungsten for the baffles and the dome. Especially the effect of a beryllium influx to the divertor targets has to be analysed.

This contribution presents ERO [2] modelling of erosion and deposition along the divertor targets

---

* Corresponding author. Fax: +49 2461 612660.
  *E-mail address:* a.kirschner@fz-juelich.de (A. Kirschner).

taking into account a constant background beryllium $Be^{2+}$ influx (0.1% or 1%) relative to the incoming deuterium ion flux along the targets. Eroded particles are followed in the modelling through the divertor plasma until they are redeposited at the divertor plates or escape from the plasma volume considered (10 cm distance from the target plates). Particles not locally redeposited are assumed to form layers at remote areas. The chemical erosion yield for graphite by deuterium impact (ions and atoms) is calculated using the latest update of the semi-empirical formula depending on the incoming deuterium flux density, surface temperature and deuterium impact energy [3]. It is assumed that $CD_4$ molecules are generated in the process of chemical erosion and released into the plasma. Ionisation and dissociation of the $CD_4$ molecules in the plasma is taken into account. Chemical erosion of redeposited carbon species is assumed to be enhanced by a factor of ten compared to the chemical erosion of graphite [4]. Physical sputtering is caused by background deuterium and beryllium ions and also by eroded impurities returning to the surface.

## 2. Basis for the ERO modelling

The plasma background for the ERO calculations is taken from B2-EIRENE calculations [5] for the reference ITER option of a carbon target with 100 MW entering the scrape-off-layer (SOL). Fig. 1 shows profiles along the divertor plates of the deuterium ion and atom flux density, electron density and temperature as function of the distance $d$ from the separatrix, where $d < 0$ corresponds to the private flux region (PFR) and $d > 0$ to the

SOL. Using these plasma parameters, chemical and physical erosion yields for pure graphite are calculated as shown in Fig. 2. For simplicity, the figures show only the erosion by deuterium ions. In the modelling also chemical and physical erosion caused by deuterium atoms and physical sputtering caused by beryllium and carbon ions is included. The figure shows also the parameters determining the chemical erosion and physical sputtering yield, i.e. the incoming deuterium ion flux, the surface temperature and the deuterium ion impact energy. The surface temperature is calculated for a CFC target of 10 mm thickness with a thermal conductivity representing average operation conditions [6]. Moving along the target from the PFR ($d < 0$) to the SOL ($d > 0$), the chemical erosion yield decreases reaching a minimum of about 0.04% for the inner and outer divertor at the location of the highest flux density. In the inner divertor, the yield increases continuously along the target moving into the SOL reaching a value of about 0.8%. In the outer divertor, a local maximum is reached at the position where the surface temperature reaches about 600 °C, but the yield decreases then due to the decrease of the surface temperature before it increases again further into the SOL up to a value of about 0.4%. Physical sputtering only occurs in the SOL whereas in the PFR the deuterium impact energy is too low (yield smaller than ~0.001% in inner and outer PFR). It is more important in the outer divertor SOL where the yield reaches about 1% for distances $d > 20$ cm from the separatrix whereas a comparable yield in the inner divertor is reached at larger distances $d > 60$ cm.
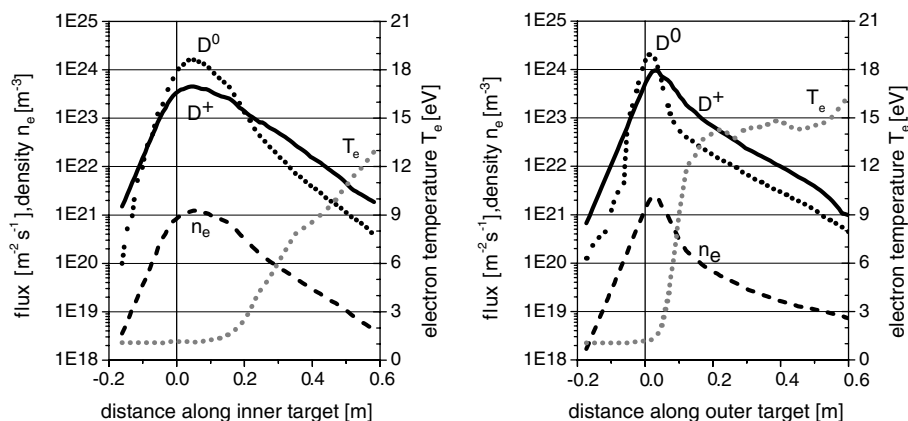


Fig. 1. Deuterium ion and atom flux, electron density and temperature along inner (left) and outer (right) divertor target plate (from B2-EIRENE).
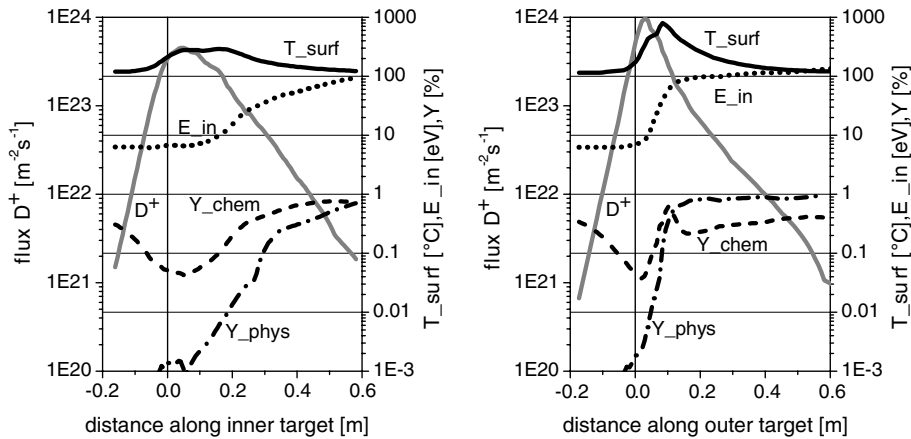
Fig. 2. Profiles of deuterium ion flux (D$^+$), surface temperature (T_surf), impact energy (E_in), chemical erosion (Y_chem) and physical sputtering yield (Y_phys) for graphite along inner (left) and outer (right) divertor plate.

## 3. ERO modelling results

### 3.1. Dynamic erosion and deposition behaviour

First, an effective sticking of zero for all hydrocarbons CD$_x$ returning to the divertor plates is assumed ($S_{eff} = 0$) [3]. The beryllium concentration in the divertor plasma is assumed to be 0.1% of the deuterium ion flux. The influence of both parameters will be discussed in Section 3.3.

The modelling starts with pure graphite target plates. Eroded carbon species which are redeposited on the target during exposure are implanted as 'cr' into the surface to distinguish them from substrate graphite ('c') particles. The surface-integrated graphite erosion rate first decreases with exposure time due to co-deposition of beryllium and redeposited carbon and approaches then a constant equilibrium value. Due to larger erosion yields and fluxes (Fig. 2) the graphite erosion is about a factor of two larger in the outer than in the inner divertor at the beginning of the exposure. The erosion rate of redeposited carbon (cr) increases from zero (there is no redeposited carbon on the surface at the beginning) to a maximum after which it decreases to an equilibrium value. Because of the assumption of a ten times enhanced chemical re-erosion of redeposited carbon compared to graphite, the overall carbon erosion (c plus cr) in equilibrium is larger than the carbon erosion at the beginning (only c) – by a factor of 2 for the outer and about 3 for the inner divertor. Obviously, a beryllium concentration of 0.1% in the edge plasma is not sufficient to build

up a protective layer which suppresses the carbon erosion significantly. Fig. 3 shows the surface concentration profiles in steady state for carbon, redeposited carbon and also beryllium along the inner and outer divertor plate. At all locations the beryllium concentration is below one indicating that no pure beryllium layer can grow which could completely suppress the carbon erosion. Around the separatrix a maximum in the beryllium surface concentration develops with a value of about 0.9 for inner and outer divertor. Here beryllium can accumulate because of the low plasma temperature preventing from physical sputtering. Deeper inside the SOL a maximum in the concentration of redeposited carbon (cr) develops (about 0.5 at the inner and 0.7 at the outer divertor plate).

In equilibrium, the amount of local redeposition of eroded carbon on the target is about 97% for the outer and 93% for the inner divertor. Particles which are not locally redeposited on the targets leave the simulation volume in the direction of the PFR and are supposed to be redeposited at remote locations. The profiles along the divertor targets after 30 s plasma exposure of net deposition/erosion, i.e. redeposited carbon (cr) plus deposited beryllium minus erosion of graphite (c), redeposited carbon (cr) and beryllium, are shown in Fig. 4. At locations inside the SOL with distances to the separatrix larger than $d \sim 0.3$ m for the inner and larger than $d \sim 0.2$ m for the outer divertor net erosion occurs. The net erosion rates at the maxima are about $1.5 \times 10^{20}$ particles/[m$^2$s] for the inner and about $2 \times 10^{20}$ particles/[m$^2$s] for the outer divertor.
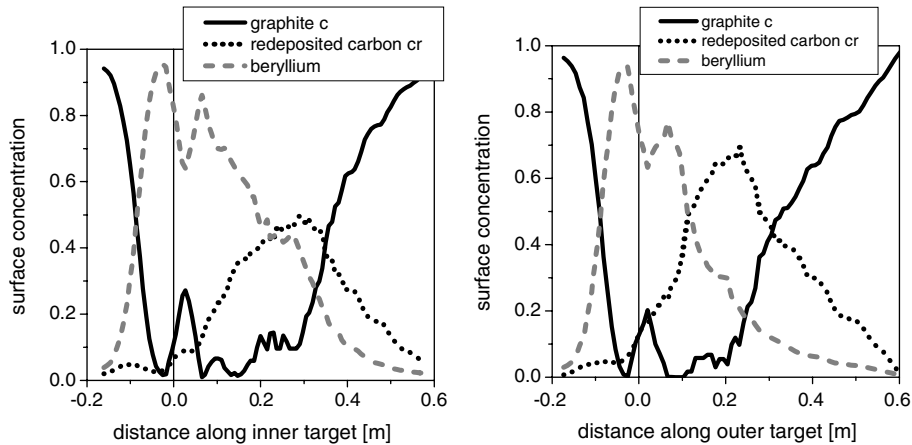
Fig. 3. Surface concentration profiles along inner (left) and outer (right) divertor for graphite, redeposited carbon and beryllium.
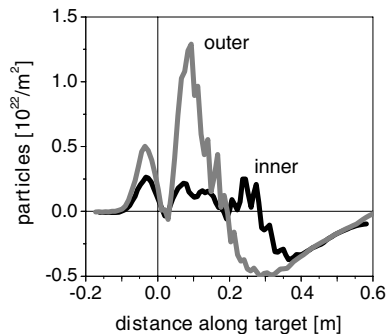


Fig. 4. Profiles of net erosion/deposition after 30 s along inner and outer divertor target.

### 3.2. Estimations of tritium retention and target lifetime

All particles which are not redeposited locally at the targets are assumed to form layers at remote areas. Therefore, the following estimations of tritium retention are upper limits. Furthermore it is assumed that carbon layers, which are built up at remote areas have a tritium content of 50%, whereas carbon layers at plasma facing components (i.e. at the divertor targets) retain a smaller tritium content of 5% [7]. For tritium which is retained by co-deposition with beryllium, a tritium to beryllium ratio $T/Be = 0.05$ is assumed [8]. Keeping the assumptions used in Section 3.1 for the effective sticking of hydrocarbons ($S_{eff} = 0$) and the beryllium concentration in the edge plasma (0.1%) the tritium retention in remote carbon layers is estimated to 4.6 mg T/s and in layers on the targets to about 0.3 mg T/s. Inner and outer divertor contribute similar amounts to the overall tritium retention in

carbon layers. Tritium retention due to beryllium deposition can be assessed to about 1.5 mg T/s resulting in an overall retention rate of 6.4 mg T/s. From this the number of discharges after which the safety limit of 350 g tritium retention is reached would be 140 based on a pulse length of 400 s.

The target lifetime can be assessed using the calculated profiles of net erosion and deposition. Taking the maximum net erosion rate of $\sim 2 \times 10^{20}$ particles/[m$^2$s] occurring at the outer divertor plate and assuming a particle density of 0.1136 atoms/Å$^3$ for graphite an erosion rate of $\sim$1.8 nm/s is estimated. Defining the lifetime as the time after which 0.5 cm material is eroded leads to about 6900 possible ITER discharges before a replacement of the divertor plate would be necessary. Compared to the number of discharges after which the safety limit of tritium retention is reached, the target lifetime problem is thus much less critical.

### 3.3. Parameter variations

Keeping the assumption of zero sticking for hydrocarbons but assuming 1% beryllium in the divertor edge plasma instead of 0.1% leads to a drastic change in the particle balances. The higher beryllium influx is now sufficient to build up expanded regions around the separatrix of pure beryllium layers which cover the underlying graphite. As result – opposite to the 0.1% beryllium case – the overall carbon erosion (c plus cr) in steady state is smaller than the graphite erosion at the beginning although redeposited carbon suffers in this calculation from a ten times enhanced chemical erosion compared to graphite. In the inner divertor the reduction is about a factor of two and in the outer about three.

Table 1
Estimated tritium retention rates

|  |  | Effective sticking $S_{eff} = 0$ | Effective sticking $S_{eff} = 1$ |
|---|---|---|---|
| **0.1% Be** | T in carbon layers | 4.9 mg T/s | 3.7 mg T/s |
|  | T in beryllium layers | 1.5 mg T/s | 1.5 mg T/s |
| **1% Be** | T in carbon layers | 1.1 mg T/s | 0.6 mg T/s |
|  | T in beryllium layers | 14.8 mg T/s | 14.8 mg T/s |

However, the amount of tritium retention increases by a factor of about 2.5. This is due to the fact that the tritium retention caused by redeposited carbon is reduced (factor ~5) while at the same time the contribution of retention by deposited beryllium increases by a factor of 10 and dominates the overall retention rate. The lifetime increases by a factor of about five with increased beryllium concentration. In addition to the larger beryllium deposition, the carbon concentration in the surface reduces naturally with increasing beryllium plasma concentration. Both effects reduce the resulting net erosion. More details of the modelling assuming 1% beryllium in the edge plasma can be found in [9]. Table 1 summarises the estimated values of tritium retention. It includes for comparison also the results if the effective sticking of hydrocarbons is changed to one. As can be seen the tritium retention decreases with $S_{eff} = 1$ although the variations are relatively small because the parameter $S_{eff}$ is only applied for molecular species whereas for atomic species always reflection coefficients from molecular dynamic calculations are used. The local redeposition on the target in steady state increases to 97% in the inner and 98.8% in the outer divertor. Therefore the lifetime also increases and is even less critical as already with $S_{eff} = 0$.

## 4. Conclusion

The modelling shows that the long-term tritium retention is much more critical than target lifetime. According to simulations of hydrocarbon transport and redeposition in fusion environments (e.g [3]) the effective sticking of hydrocarbons at plasma-wetted areas is assumed to be negligible, $S_{eff} = 0$. Using this assumption, the modelling shows upper values of tritium retention rates of 6.4 mg T/s with 0.1% Be in the divertor edge plasma and 15.9 mg T/s for

1% Be. Assuming, for comparison, a first wall made of carbon with a carbon influx into the divertor of 1% relative to the deuterium ion flux, a larger retention rate of about 32 mg T/s would be obtained. Former estimations without Be influx [3] led to a retention rate of about 1 mg T/s assuming $S_{eff} = 0$. Therefore, there seems to be no significant reduction due to the beryllium co-deposition. Main reason for this is the ten times enhanced chemical re-erosion of redeposited carbon taken into account for the present modelling. Furthermore, in the past a T/C ratio of 0.2 has been assumed for remotely deposited carbon layers instead of 0.5. Also, tritium retention in locally deposited layers on the targets has not been taken into account.

For all estimations of tritium retention, one has to keep in mind that the influence of transient heat loads such as ELMs or disruptions on the stability of the formed redeposited and protective layers is not considered here. The beneficial effect of reduction of carbon erosion due to the coverage with beryllium could vanish if the beryllium layers do not withstand such heat loads. In addition, deposition of carbon inside gaps between the castellated divertor plates is not considered in the calculations presented here. On the other hand, the co-deposition of beryllium could suppress the erosion of carbon not only due to dilution of carbon in the surface. As observed in PISCES-B experiments [10] the formation of carbides further reduces the carbon erosion. Taking into account such effects for the ITER modelling would result in a decrease of tritium retention. The sticking of carbon species at shadowed and remote areas was assumed to be one. This of course is an upper value whereby in reality part of these species can be pumped out without sticking inside the machine and therefore reducing the in-vessel tritium inventory.

## References

[1] ITER Technical Basis, ITER EDA Documentation Series No. 24, IAEA Vienna, 2002.
[2] A. Kirschner et al., Nucl. Fus. 40 (5) (2000) 989.
[3] J. Roth et al., J. Nucl. Mater. 337–339 (2005) 970.
[4] A. Kirschner et al., J. Nucl. Mater. 328 (2004) 62.
[5] G. Federici et al., J. Nucl. Mater. 313–316 (2003) 11.
[6] G. Federici, A. Loarte, G. Strohmayer, Plasma Phys. Control. Fus., 45 (2003) 1523.
[7] J. von Seggern et al., J. Nucl. Mater. 313–316 (2003) 439.
[8] M.J. Baldwin, J. Nucl. Mater. 337–339 (2005) 590.
[9] A. Kirschner et al., EPS Conference 2005, ECA Vol. 29C, P-1.013, Tarragona, Spain (2005).
[10] M.J. Baldwin, R.P. Doerner, Nucl. Fusion 46 (2006) 444.